AIP | The Journal of Chemical Physics

Real-space computation of dynamic hyperpolarizabilities

J.-I. Iwata, K. Yabana, and G. F. Bertsch

Citation: J. Chem. Phys. **115**, 8773 (2001); doi: 10.1063/1.1411996
View online: http://dx.doi.org/10.1063/1.1411996
View Table of Contents: http://jcp.aip.org/resource/1/JCPSA6/v115/i19
Published by the American Institute of Physics.

Real-space computation of dynamic hyperpolarizabilities

J.-I. Iwata[a] and K. Yabana[b]
Institute of Physics, University of Tsukuba, Tsukuba 305-8571, Japan

G. F. Bertsch[c]
Department of Physics and National Institute for Nuclear Theory, University of Washington, Seattle, Washington 98195

(Received 29 June 2001; accepted 24 August 2001)

A real-space method is developed to calculate molecular hyperpolarizabilities in the time-dependent density functional theory. The method is based on the response function formalism which was developed by Senatore and Subbaswamy for the third harmonic generation of rare-gas atoms [Phys. Rev. A **35**, 2440 (1987)]. The response equations are discretized in real space employing a uniform grid representation in the three-dimensional Cartesian coordinate, and are solved with iterative methods such as conjugate-gradient and conjugate-residual methods. The method works efficiently for both small and large molecules, and for any nonlinear optical processes up to third order. The spatial convergence of the calculation can be examined with two intuitive parameters, the grid spacing and the spatial box size. Applications of our method are presented for rare-gas atoms and molecules, N_2, H_2O, C_2H_4, C_6H_6, and C_{60}. Our results agree well with other calculations employing basis functions except for a slight deviation in a large molecule, C_{60}. © *2001 American Institute of Physics.* [DOI: 10.1063/1.1411996]

I. INTRODUCTION

In recent years, molecules with large hyperpolarizabilities, especially organic and polymeric ones, have been attracting considerable interest for their possible usefulness as nonlinear optical materials.[1] In theoretical side, *ab initio* as well as empirical methods have been extensively employed,[2] but more efficient methods are needed for a quantitative theory in large molecules. These methods should take account of electronic correlations, frequency dispersion, and an appropriate choice of the basis functions.[3,4]

To include electronic correlation effects in the excitation of molecules and condensed matter, the time-dependent density functional theory (TD-DFT) gives a simple description with reasonable accuracy. The TD-DFT is an extension of the static density functional theory (DFT) to describe electronic dynamics under a time-dependent external field.[5] Electronic correlations are usually treated by a simple procedure using the adiabatic local density approximation (ALDA). The theory has been applied to excited states of molecules,[6,7] linear optical responses,[7–12] and collision phenomena.[13,14] The first application of the TD-DFT to nonlinear response was made by Senatore and Subbaswamy who calculated hyperpolarizability of rare gas atoms.[15] The nonlinear susceptibility of bulk semiconductors was calculated next.[16,17] Recently, van Gisbergen *et al.* have extensively investigated the dynamic hyperpolarizabilities of molecules.[18,19] Their results show that the TD-DFT is a promising tool to investigate nonlinear optical properties of molecules.

The representation of the electron wave functions or the choice of basis orbitals is an important aspect in the calculations of molecular hyperpolarizabilities. When using basis functions, it is well known that many more diffuse functions are required to obtain converged results for the hyperpolarizability than for the ground state.[4] An alternative to basis functions is a grid representation in the three-dimensional Cartesian coordinate.[20–23] In the local density approximation (LDA), the real-space representation is especially convenient because the Hamiltonian is almost diagonal in the real-space representation. Another attractive feature of the grid representation is that the numerical convergence can be easily checked. The convergence is controlled by two intuitively transparent parameters, the mesh spacing and the volume of the computational grid. The grid representation has been already applied to calculation of the static hyperpolarizability in Ref. 24.

The grid representation has been utilized in calculating the linear response calculation of molecules (see Ref. 25 for a frequency-domain treatment and Ref. 9 for a real-time implementation). The real-time method is useful to efficiently describe optical response of whole spectral region. However, the real-time method may not be the best technique outside the applications to linear response and response to very large fields. In the present work, we employ the frequency-domain response function formalism.[15] Combined with the modified Sternheimer method,[26] the molecular hyperpolarizabilities can be efficiently calculated in the grid representation. The method was briefly explained in Ref. 27. A similar method has been utilized for the nonlinear susceptibilities in solids.[17]

The paper is organized as follows. In Sec. II, we present general response function formalism capable of describing any kinds of nonlinear optical processes up to third order by extending the response formalism of Ref. 15. In Sec. III,

[a]Electronic mail: iwata@nucl.ph.tsukuba.ac.jp
[b]Electronic mail: yabana@nucl.ph.tsukuba.ac.jp
[c]Electronic mail: bertsch@phys.washington.edu

computational details are discussed to solve response equations. In Sec. IV, we present calculated results of hyperpolarizabilities for some rare-gas atoms (Ne, Ar, Kr), small molecules (N_2, H_2O, C_2H_4), benzene, and C_{60}. In Sec. V, we summarize our findings.

II. TIME-DEPENDENT DENSITY FUNCTIONAL THEORY FOR NONLINEAR RESPONSE FUNCTIONS

A. Definition of hyperpolarizabilities

We first define the hyperpolarizabilities of interest.[28] The dipole moment $\mathbf{p}(t)$ induced by an external electric field $\mathbf{E}(t)$ of moderate intensity is expressed in a power series as

$$\mathbf{p}(t)=\mathbf{p}^{(0)}(t)+\mathbf{p}^{(1)}(t)+\mathbf{p}^{(2)}(t)+\mathbf{p}^{(3)}(t)+\ldots, \tag{1}$$

where $\mathbf{p}^{(1)}(t)$ is linearly dependent, $\mathbf{p}^{(2)}(t)$ is quadratically dependent on the external field, and so on. When the external field is a superposition of monochromatic waves

$$\mathbf{E}(t)=\frac{1}{2}\sum_{\omega_i\geqslant 0}\{\mathbf{E}_{\omega_i}e^{-i\omega_i t}+\mathbf{E}_{-\omega_i}e^{i\omega_i t}\}, \tag{2}$$

$\mathbf{p}^{(n)}(t)$ can be expressed in a similar form

$$\mathbf{p}^{(n)}(t)=\frac{1}{2}\sum_{\omega_\sigma\geqslant 0}\{\mathbf{p}^{(n)}_{\omega_\sigma}e^{-i\omega_\sigma t}+\mathbf{p}^{(n)}_{-\omega_\sigma}e^{i\omega_\sigma t}\}, \tag{3}$$

where the Cartesian μ-component of $\mathbf{p}^{(n)}_{\omega_\sigma}$ is given by

$$\begin{aligned}(\mathbf{p}^{(n)}_{\omega_\sigma})_\mu=&\frac{1}{n!}\sum_{\alpha_1,\ldots,\alpha_n}\sum_{\{\omega_1,\ldots,\omega_n\}}K(-\omega_\sigma;\omega_1,\ldots,\omega_n)\\&\times\chi^{(n)}_{\mu\alpha_1\ldots\alpha_n}(-\omega_\sigma;\omega_1,\ldots,\omega_n)\\&\times(\mathbf{E}_{\omega_1})_{\alpha_1}\ldots(\mathbf{E}_{\omega_n})_{\alpha_n}.\end{aligned} \tag{4}$$

$\chi^{(n)}_{\mu\alpha_1\ldots\alpha_n}(-\omega_\sigma;\omega_1,\ldots,\omega_n)$ is the so-called n-th order nonlinear polarizability tensor or $(n-1)$-th order hyperpolarizability tensor. The sum $\Sigma_{\{\omega_1,\ldots,\omega_n\}}$ is taken over all distinct sets of $\{\omega_1,\ldots,\omega_n\}$ whose sum is equal to ω_σ. $K(-\omega_\sigma;\omega_1,\ldots,\omega_n)$ is a numerical factor defined as

$$K(-\omega_\sigma;\omega_1,\ldots,\omega_n)=2^{l+m-n}p, \tag{5}$$

where p is the number of distinct permutations of $\{\omega_1,\ldots,\omega_n\}$, n is the order of nonlinearity, and m is the number of frequencies which are equal to zero. $l=1$ if $\omega_\sigma\neq 0$, otherwise $l=0$.

Usually, nonlinear optical processes up to third order are of interest. The first-, second-, and third-order polarizabilities are expressed by the special symbols, $\alpha(-\omega_1;\omega_1)$, $\beta(-\omega_\sigma;\omega_1,\omega_2)$, $\gamma(-\omega_\sigma;\omega_1,\omega_2,\omega_3)$, respectively. Some processes have their own names which originate from the relevant physical phenomena. For the second-order processes, $\beta(0;\omega,-\omega)$ and $\beta(-2\omega;\omega,\omega)$ correspond to the optical rectification (OR) and the second-harmonic generation (SHG), respectively. For the third-order processes, $\gamma(-\omega;0,0,\omega)$ corresponds to the electro-optic Kerr effect (EOKE). $\gamma(-\omega;\omega,-\omega,\omega)$ corresponds to the intensity-dependent refractive index (IDRI) or degenerate four-wave mixing. $\gamma(-2\omega;0,\omega,\omega)$ corresponds to the electric field-induced second-harmonic generation (EFISH), and $\gamma(-3\omega;\omega,\omega,\omega)$ corresponds to the third-harmonic generation (THG).

B. Response function formalism

In this section, the response function formalism based on the TD-DFT[15] is presented for general nonlinear responses up to third order.

The time evolution of a system under the external field Eq. (2) is described by the time-dependent Kohn–Sham equation,[5]

$$i\hbar\frac{\partial}{\partial t}\psi_i(\mathbf{r},t)=(h[\rho](\mathbf{r},t)+v^{ext}(\mathbf{r},t))\psi_i(\mathbf{r},t), \tag{6}$$

$$\begin{aligned}h[\rho](\mathbf{r},t)=&\frac{-\hbar^2}{2m}\nabla^2+V_{ion}(\mathbf{r})\\&+e^2\int d\mathbf{r}'\frac{\rho(\mathbf{r}',t)}{|\mathbf{r}-\mathbf{r}'|}+V_{xc}[\rho](\mathbf{r},t),\end{aligned} \tag{7}$$

$$\rho(\mathbf{r},t)=\sum_i^{occ.}|\psi_i(\mathbf{r},t)|^2. \tag{8}$$

In the dipole approximation, the external perturbation $v^{ext}(\mathbf{r},t)$ can be written as

$$v^{ext}(\mathbf{r},t)=\frac{1}{2}\sum_{\omega_i\geqslant 0}\{v^{ext}_{\omega_i}(\mathbf{r})e^{-i\omega_i t}+v^{ext}_{-\omega_i}(\mathbf{r})e^{i\omega_i t}\}, \tag{9}$$

$$\begin{aligned}v^{ext}_{\omega_i}(\mathbf{r})=&\sum_{\alpha=x,y,z}er_\alpha(\mathbf{E}_{\omega_i})_\alpha\\\equiv&\sum_{\alpha=x,y,z}v^{ext}_\alpha(\mathbf{r}|-\omega_i;\omega_i)(\mathbf{E}_{\omega_i})_\alpha.\end{aligned} \tag{10}$$

For sufficiently small external perturbation, one may expand the single-particle density $\rho(\mathbf{r},t)$ and the Kohn–Sham Hamiltonian $h[\rho]$ as

$$\rho(\mathbf{r},t)=\rho^{(0)}(\mathbf{r})+\rho^{(1)}(\mathbf{r},t)+\rho^{(2)}(\mathbf{r},t)+\rho^{(3)}(\mathbf{r},t)+\ldots, \tag{11}$$

$$\begin{aligned}h[\rho](\mathbf{r},t)=&h[\rho^{(0)}](\mathbf{r})+h^{(1)}(\mathbf{r},t)+h^{(2)}(\mathbf{r},t)\\&+h^{(3)}(\mathbf{r},t)+\ldots.\end{aligned} \tag{12}$$

$\rho^{(n)}(\mathbf{r},t)$ and $h^{(n)}(\mathbf{r},t)$ have similar forms as Eq. (9)

$$\rho^{(n)}(\mathbf{r},t)=\frac{1}{2}\sum_{\omega_\sigma\geqslant 0}\{\rho^{(n)}_{\omega_\sigma}(\mathbf{r})e^{-i\omega_\sigma t}+\rho^{(n)}_{-\omega_\sigma}(\mathbf{r})e^{i\omega_\sigma t}\}, \quad (13)$$

$$h^{(n)}(\mathbf{r},t)=\frac{1}{2}\sum_{\omega_\sigma\geqslant 0}\{h^{(n)}_{\omega_\sigma}(\mathbf{r})e^{-i\omega_\sigma t}+h^{(n)}_{-\omega_\sigma}(\mathbf{r})e^{i\omega_\sigma t}\}, \quad (14)$$

where

$$\rho^{(n)}_{\omega_\sigma}(\mathbf{r})=\frac{1}{n!}\sum_{\alpha_1,\ldots,\alpha_n}\sum_{\{\omega_1,\ldots,\omega_n\}}K(-\omega_\sigma;\omega_1,\ldots,\omega_n)\times\rho^{(n)}_{\alpha_1\ldots\alpha_n}(\mathbf{r}|-\omega_\sigma;\omega_1,\ldots,\omega_n)\times(\mathbf{E}_{\omega_1})_{\alpha_1}\ldots(\mathbf{E}_{\omega_n})_{\alpha_n}, \quad (15)$$

$$h^{(n)}_{\omega_\sigma}(\mathbf{r})=\frac{1}{n!}\sum_{\alpha_1,\ldots,\alpha_n}\sum_{\{\omega_1,\ldots,\omega_n\}}K(-\omega_\sigma;\omega_1,\ldots,\omega_n)\times h^{(n)}_{\alpha_1\ldots\alpha_n}(\mathbf{r}|-\omega_\sigma;\omega_1,\ldots,\omega_n)(\mathbf{E}_{\omega_1})_{\alpha_1}\ldots(\mathbf{E}_{\omega_n})_{\alpha_n}. \quad (16)$$

The $(n-1)$-th order hyperpolarizability tensor is related to the n-th order transition density $\rho^{(n)}_{\alpha_1\ldots\alpha_n}(\mathbf{r}|-\omega_\sigma;\omega_1,\ldots,\omega_n)$ by

$$\chi^{(n)}_{\mu\alpha_1\ldots\alpha_n}(-\omega_\sigma;\omega_1,\ldots,\omega_n)=-e\int d\mathbf{r}r_\mu\rho^{(n)}_{\alpha_1\ldots\alpha_n}(\mathbf{r}|-\omega_\sigma;\omega_1,\ldots,\omega_n). \quad (17)$$

Since we are interested in hyperpolarizabilities of first three orders in Eq. (17), which are linear polarizability $\alpha(-\omega_1;\omega_1)$, first and second hyperpolarizabilities, $\beta(-\omega_\sigma;\omega_1,\omega_2)$ and $\gamma(-\omega_\sigma;\omega_1,\omega_2,\omega_3)$, we need to calculate transition densities $\rho^{(n)}_{\alpha_1\ldots\alpha_n}(\mathbf{r}|-\omega_\sigma;\omega_1,\ldots,\omega_n)$ up to third order.

Putting Eqs. (9)–(16) into Eqs. (6)–(8) and applying the time-dependent perturbation theory, one can obtain the following equations for the transition densities. The first-order equation is the linear response equation,[8]

$$\rho^{(1)}_{\alpha_1}(\mathbf{r}|-\omega_\sigma;\omega_\sigma)=\int d\mathbf{r}'\,\chi^{(1)}(\mathbf{r},\mathbf{r}';\omega_\sigma)\times h^{(1)}_{\alpha_1}(\mathbf{r}'|-\omega_\sigma;\omega_\sigma), \quad (18)$$

$$h^{(1)}_{\alpha_1}(\mathbf{r}|-\omega_\sigma;\omega_\sigma)=\int d\mathbf{r}'\left\{\frac{e^2}{|\mathbf{r}-\mathbf{r}'|}+f_{xc}(\mathbf{r},\mathbf{r}';\omega_\sigma)\right\}\times\rho^{(1)}_{\alpha_1}(\mathbf{r}'|-\omega_\sigma;\omega_\sigma)+v^{ext}_{\alpha_1}(\mathbf{r}|-\omega_\sigma;\omega_\sigma), \quad (19)$$

where $\chi^{(1)}$ is the first-order independent-particle response function which is expressed as,[8,15]

$$\chi^{(1)}(\mathbf{r},\mathbf{r}';\omega_\sigma)=\sum_i^{occ.}\{\phi_i^*(\mathbf{r})\phi_i(\mathbf{r}')G^{(+)}(\mathbf{r},\mathbf{r}';\epsilon_i+\hbar\omega_\sigma)+\phi_i(\mathbf{r})\phi_i^*(\mathbf{r}')G^{(-)}(\mathbf{r}',\mathbf{r};\epsilon_i-\hbar\omega_\sigma)\}. \quad (20)$$

Here $\{\phi_i,\ \epsilon_i\}$ are the static (unperturbed) Kohn–Sham orbitals and energies, and $G^{(\pm)}$ are the single-particle Green functions,

$$G^{(\pm)}(\mathbf{r},\mathbf{r}';E)=\sum_j\frac{\phi_j(\mathbf{r})\phi_j^*(\mathbf{r}')}{E-\epsilon_j\pm i\eta}, \quad (21)$$

where η is a positive infinitesimal. f_{xc} is the first-order exchange-correlation kernel which will be explained following.

The second-order and the third-order equations can be written in a similar way. The second-order equations are

$$\rho^{(2)}_{\alpha_1\alpha_2}(\mathbf{r}|-\omega_\sigma;\omega_1,\omega_2)=\int d\mathbf{r}'\chi^{(1)}(\mathbf{r},\mathbf{r}';\omega_\sigma)h^{(2)}_{\alpha_1\alpha_2}(\mathbf{r}'|-\omega_\sigma;\omega_1,\omega_2)+\int d\mathbf{r}'d\mathbf{r}''\chi^{(2)}(\mathbf{r},\mathbf{r}',\mathbf{r}'';\omega_1,\omega_2)\times h^{(1)}_{\alpha_1}(\mathbf{r}'|-\omega_1;\omega_1)h^{(1)}_{\alpha_2}(\mathbf{r}''|-\omega_2;\omega_2), \quad (22)$$

$$h^{(2)}_{\alpha_1\alpha_2}(\mathbf{r}|-\omega_\sigma;\omega_1,\omega_2)=\int d\mathbf{r}'\left\{\frac{e^2}{|\mathbf{r}-\mathbf{r}'|}+f_{xc}(\mathbf{r},\mathbf{r}';\omega_\sigma)\right\}\times\rho^{(2)}_{\alpha_1\alpha_2}(\mathbf{r}'|-\omega_\sigma;\omega_1,\omega_2)+\int d\mathbf{r}'d\mathbf{r}''g_{xc}(\mathbf{r},\mathbf{r}',\mathbf{r}'';\omega_1,\omega_2)\times\rho^{(1)}_{\alpha_1}(\mathbf{r}'|-\omega_1;\omega_1)\rho^{(1)}_{\alpha_2}(\mathbf{r}''|-\omega_2;\omega_2). \quad (23)$$

The third-order equations are

$$\begin{aligned}
&\rho^{(3)}_{\alpha_1\alpha_2\alpha_3}(\mathbf{r}|-\omega_\sigma;\omega_1,\omega_2,\omega_3)\\
&\quad=\int d\mathbf{r}'\chi^{(1)}(\mathbf{r},\mathbf{r}';\omega_\sigma)h^{(3)}_{\alpha_1\alpha_2\alpha_3}(\mathbf{r}'|-\omega_\sigma;\omega_1,\omega_2,\omega_3)\\
&\qquad+\int d\mathbf{r}'d\mathbf{r}''\chi^{(2)}(\mathbf{r},\mathbf{r}',\mathbf{r}'';\omega_1,\omega_2+\omega_3)h^{(1)}_{\alpha_1}(\mathbf{r}'|-\omega_1;\omega_1)h^{(2)}_{\alpha_2\alpha_3}(\mathbf{r}''|-\omega_2-\omega_3;\omega_2,\omega_3)\\
&\qquad+\int d\mathbf{r}'d\mathbf{r}''\chi^{(2)}(\mathbf{r},\mathbf{r}',\mathbf{r}'';\omega_2,\omega_3+\omega_1)h^{(1)}_{\alpha_2}(\mathbf{r}'|-\omega_2;\omega_2)h^{(2)}_{\alpha_3\alpha_1}(\mathbf{r}''|-\omega_3-\omega_1;\omega_3,\omega_1)\\
&\qquad+\int d\mathbf{r}'d\mathbf{r}''\chi^{(2)}(\mathbf{r},\mathbf{r}',\mathbf{r}'';\omega_3,\omega_1+\omega_2)h^{(1)}_{\alpha_3}(\mathbf{r}'|-\omega_3;\omega_3)h^{(2)}_{\alpha_1\alpha_2}(\mathbf{r}''|-\omega_1-\omega_2;\omega_1,\omega_2)\\
&\qquad+\int d\mathbf{r}'d\mathbf{r}''d\mathbf{r}'''\chi^{(3)}(\mathbf{r},\mathbf{r}',\mathbf{r}'',\mathbf{r}''';\omega_1,\omega_2,\omega_3)h^{(1)}_{\alpha_1}(\mathbf{r}'|-\omega_1;\omega_1)h^{(1)}_{\alpha_2}(\mathbf{r}''|-\omega_2;\omega_2)h^{(1)}_{\alpha_3}(\mathbf{r}'''|-\omega_3;\omega_3),
\end{aligned}\tag{24}$$

$$\begin{aligned}
&h^{(3)}_{\alpha_1\alpha_2\alpha_3}(\mathbf{r}|-\omega_\sigma;\omega_1,\omega_2,\omega_3)\\
&\quad=\int d\mathbf{r}'\left\{\frac{e^2}{|\mathbf{r}-\mathbf{r}'|}+f_{xc}(\mathbf{r},\mathbf{r}';\omega_\sigma)\right\}\rho^{(3)}_{\alpha_1\alpha_2\alpha_3}(\mathbf{r}'|-\omega_\sigma;\omega_1,\omega_2,\omega_3)\\
&\qquad+\int d\mathbf{r}'d\mathbf{r}''g_{xc}(\mathbf{r},\mathbf{r}',\mathbf{r}'';\omega_1,\omega_2+\omega_3)\rho^{(1)}_{\alpha_1}(\mathbf{r}'|-\omega_1;\omega_1)\rho^{(2)}_{\alpha_2\alpha_3}(\mathbf{r}''|-\omega_2-\omega_3;\omega_2,\omega_3)\\
&\qquad+\int d\mathbf{r}'d\mathbf{r}''g_{xc}(\mathbf{r},\mathbf{r}',\mathbf{r}'';\omega_2,\omega_3+\omega_1)\rho^{(1)}_{\alpha_2}(\mathbf{r}'|-\omega_2;\omega_2)\rho^{(2)}_{\alpha_3\alpha_1}(\mathbf{r}''|-\omega_3-\omega_1;\omega_3,\omega_1)\\
&\qquad+\int d\mathbf{r}'d\mathbf{r}''g_{xc}(\mathbf{r},\mathbf{r}',\mathbf{r}'';\omega_3,\omega_1+\omega_2)\rho^{(1)}_{\alpha_3}(\mathbf{r}'|-\omega_3;\omega_3)\rho^{(2)}_{\alpha_1\alpha_2}(\mathbf{r}''|-\omega_1-\omega_2;\omega_1,\omega_2)\\
&\qquad+\int d\mathbf{r}'d\mathbf{r}''d\mathbf{r}'''h_{xc}(\mathbf{r},\mathbf{r}',\mathbf{r}'',\mathbf{r}''';\omega_1,\omega_2,\omega_3)\rho^{(1)}_{\alpha_1}(\mathbf{r}'|-\omega_1;\omega_1)\rho^{(1)}_{\alpha_2}(\mathbf{r}''|-\omega_2;\omega_2)\rho^{(1)}_{\alpha_3}(\mathbf{r}'''|-\omega_3;\omega_3).
\end{aligned}\tag{25}$$

Here $\chi^{(2)}$ and $\chi^{(3)}$ are the second- and third-order independent-particle response functions which can be written as follows,[15]

$$\begin{aligned}
\chi^{(2)}(\mathbf{r},\mathbf{r}_1,\mathbf{r}_2;\omega_1,\omega_2)=\sum_i^{occ.}\{&\phi_i^*(\mathbf{r})\phi_i(\mathbf{r}_2)G^{(+)}(\mathbf{r},\mathbf{r}_1;\hbar(\omega_1+\omega_2)+\epsilon_i)G^{(+)}(\mathbf{r}_1,\mathbf{r}_2;\hbar\omega_2+\epsilon_i)\\
&+\phi_i(\mathbf{r})\phi_i^*(\mathbf{r}_2)G^{(-)}(\mathbf{r}_1,\mathbf{r};-\hbar(\omega_1+\omega_2)+\epsilon_i)G^{(-)}(\mathbf{r}_2,\mathbf{r}_1;-\hbar\omega_2+\epsilon_i)\\
&+\phi_i^*(\mathbf{r}_1)\phi_i(\mathbf{r}_2)G^{(-)}(\mathbf{r}_1,\mathbf{r};-\hbar\omega_1+\epsilon_i)G^{(+)}(\mathbf{r},\mathbf{r}_2;\quad\hbar\omega_2+\epsilon_i)+\text{permutations of }(\mathbf{r}_1\omega_1;\mathbf{r}_2\omega_2)\},
\end{aligned}\tag{26}$$

$$\begin{aligned}
&\chi^{(3)}(\mathbf{r},\mathbf{r}_1,\mathbf{r}_2,\mathbf{r}_3;\omega_1,\omega_2,\omega_3)\\
&\quad=\sum_i^{occ.}\{\phi_i^*(\mathbf{r})\phi_i(\mathbf{r}_3)G^{(+)}(\mathbf{r},\mathbf{r}_1;\hbar(\omega_1+\omega_2+\omega_3)+\epsilon_i)G^{(+)}(\mathbf{r}_1,\mathbf{r}_2;\hbar(\omega_2+\omega_3)+\epsilon_i)G^{(+)}(\mathbf{r}_2,\mathbf{r}_3;\hbar\omega_3+\epsilon_i)\\
&\qquad+\phi_i(\mathbf{r})\phi_i^*(\mathbf{r}_3)G^{(-)}(\mathbf{r}_1,\mathbf{r};-\hbar(\omega_1+\omega_2+\omega_3)+\epsilon_i)G^{(-)}(\mathbf{r}_2,\mathbf{r}_1;-\hbar(\omega_2+\omega_3)+\epsilon_i)G^{(-)}(\mathbf{r}_3,\mathbf{r}_2;-\hbar\omega_3+\epsilon_i)\\
&\qquad+\phi_i^*(\mathbf{r}_1)\phi_i(\mathbf{r}_3)G^{(-)}(\mathbf{r}_1,\mathbf{r};-\hbar\omega_1+\epsilon_i)G^{(+)}(\mathbf{r},\mathbf{r}_2;\hbar(\omega_2+\omega_3)+\epsilon_i)G^{(+)}(\mathbf{r}_2,\mathbf{r}_3;\hbar\omega_3+\epsilon_i)\\
&\qquad+\phi_i(\mathbf{r}_1)\phi_i^*(\mathbf{r}_3)G^{(+)}(\mathbf{r},\mathbf{r}_1;\hbar\omega_1+\epsilon_i)G^{(-)}(\mathbf{r}_2,\mathbf{r};-\hbar(\omega_2+\omega_3)+\epsilon_i)G^{(-)}(\mathbf{r}_3,\mathbf{r}_2;-\hbar\omega_3+\epsilon_i)\\
&\qquad+\text{all permutations of }(\mathbf{r}_1\omega_1;\mathbf{r}_2\omega_2;\mathbf{r}_3\omega_3)\}.
\end{aligned}\tag{27}$$

The second- and the third-order exchange-correlation kernels are g_{xc} and h_{xc}, respectively.

In the TD-DFT, exchange and correlation effects are included in $V_{xc}[\rho]$ and its functional derivatives, f_{xc}, g_{xc}, and h_{xc}, which are called the exchange-correlation kernels.[5] In practical calculations, one usually makes the adiabatic approximation, in which the same exchange-correlation functional is used as in the static problem. In the calculations below, we assume the adiabatic local-density approximation (ALDA). In the ALDA, the exchange-correlation kernels are given as follows:[5,19]

$$f_{xc}(\mathbf{r},\mathbf{r}';\omega)=\left.\frac{dV_{xc}^{LDA}}{d\rho}\right|_{\rho^{(0)}}\delta(\mathbf{r}-\mathbf{r}'), \tag{28}$$

$$g_{xc}(\mathbf{r},\mathbf{r}',\mathbf{r}'';\omega_1,\omega_2)=\left.\frac{d^2V_{xc}^{LDA}}{d\rho^2}\right|_{\rho^{(0)}}\delta(\mathbf{r}-\mathbf{r}')\,\delta(\mathbf{r}'-\mathbf{r}''), \tag{29}$$

$$h_{xc}(\mathbf{r},\mathbf{r}',\mathbf{r}'',\mathbf{r}''';\omega_1,\omega_2,\omega_3)=\left.\frac{d^3V_{xc}^{LDA}}{d\rho^3}\right|_{\rho^{(0)}}\delta(\mathbf{r}-\mathbf{r}')\,\delta(\mathbf{r}'-\mathbf{r}'')\,\delta(\mathbf{r}''-\mathbf{r}'''). \tag{30}$$

III. REAL-SPACE COMPUTATIONAL METHOD

In this section, we present a procedure to solve response equations in real space. This procedure is an extension of the method for linear response[7] and was explained briefly in Ref. 27. From now on, we will only consider the cases where the frequencies of external fields are far below the excitation energy of the first excited state, and assume that all quantities (wave functions, Green functions, etc.) are real functions.

A. Hamiltonian and ground-state calculation

First the ground state is constructed by solving the static Kohn–Sham equation,

$$h[\rho^{(0)}]\phi_i(\mathbf{r})=\epsilon_i\phi_i(\mathbf{r}), \tag{31}$$

$$\begin{aligned}h[\rho^{(0)}](\mathbf{r})&=\frac{-\hbar^2}{2m}\nabla^2+\hat{V}_{ion}\\&\quad+\int d\mathbf{r}'\frac{e^2}{|\mathbf{r}-\mathbf{r}'|}\rho^{(0)}(\mathbf{r}')+V_{xc}[\rho^{(0)}](\mathbf{r}),\\ \rho^{(0)}(\mathbf{r})&=\sum_{i}^{occ.}|\phi_i(\mathbf{r})|^2.\end{aligned} \tag{32}$$

In solving the equation, the wave functions and potentials are discretized employing a uniform grid representation in the three-dimensional Cartesian coordinate. Grid points inside a sphere of a certain radius are used. The wave functions are put to zero outside the box. The kinetic energy operator is treated by a higher-order finite difference approximation.[20] The electron-ion interactions are described with norm-conserving pseudopotentials[29] in the separable approximation.[30] Since only valence electrons are treated explicitly, polarization effects of the core electrons are ignored in the response calculation. The pseudopotentials are generated from the LDA calculation of atoms. For rare gas atoms, Ne, Ar, Kr, *s*- and *p*-electrons are treated as valence, and the ionic core radii in the pseudopotential construction are chosen as 1.37, 1.05, and 1.05 Å, respectively. Partial waves of *s, p, d* are included in the nonlocal part of the pseudopotentials. For elements H, C, N, O, the ionic core radius is chosen as 0.8 Å, and partial waves of *s* and *p* are included. The Hartree potential is calculated by solving the Poisson equation where the boundary values are generated by making a multipole expansion of density.

Several kinds of exchange-correlation potential will be employed. They include the LDA, the generalized gradient approximation (GGA), and the asymptotically corrected potential (AC). The LDA potential with Perdew–Zunger (PZ) parameterization[31] is used for rare- gas atoms. Vosko–Wilk–Nusair (VWN) parameterization[32] is used for molecules. As a standard GGA functional, the BLYP potential is used, which is a combination of Becke's exchange and Lee–Yang–Parr's correlation functional.[33,34] For descriptions of excited states as well as electronic responses, it has been recognized that the AC potential[35,36] substantially improves the LDA results. We employ the AC potential LB94 proposed by Leeuwen and Baerends.[35] These functionals are only used as exchange-correlation potential in the ground state calculations. It has been argued that the nonlinear response is not sensitive to the choice of the exchange-correlation kernels.[19] To compare our results directly with the previous one in which the difference in the exchange-correlation kernels is ignored,[19] we use the ALDA exchange-correlation kernels irrespective of the potential which is used in the ground-state calculation.

B. Nonlinear response calculations

From Eqs. (18), (22), and (24), we see that the response equations can be expressed generally as follows:

$$\begin{aligned}&\rho^{(n)}_{\alpha_1\cdots\alpha_n}(\mathbf{r}|-\omega_\sigma;\omega_1,\ldots,\omega_n)\\&\quad=\int d\mathbf{r}'\chi^{(1)}(\mathbf{r},\mathbf{r}';\omega_\sigma)\int d\mathbf{r}''\left\{\frac{e^2}{|\mathbf{r}'-\mathbf{r}''|}+f_{xc}(\mathbf{r}',\mathbf{r}'';\omega_\sigma)\right\}\\&\qquad\times\rho^{(n)}_{\alpha_1\cdots\alpha_n}(\mathbf{r}''|-\omega_\sigma;\omega_1,\ldots,\omega_n)+b^{(n-1)}(\mathbf{r}),\end{aligned} \tag{33}$$

where $b^{(n-1)}(\mathbf{r})$ is a collection of terms involving quantities up to $(n-1)$-th order. Thus the response equation of any order has the same structure as that of the linear response, Eq. (18).[5] These response equations can be solved efficiently in real space with the modified Sternheimer method.[7,26]

In the grid representation, Eq. (33) is a linear algebraic equation for an unknown vector $\rho^{(n)}(i)$ $(i=1,\ldots,M)$ where M is the number of grid points. This equation can be solved efficiently with an iterative procedure for a linear-algebraic equation with real nonsymmetric matrix, such as the conjugate-residual (CR) method.[37] Equation (33) includes integrals involving the response function $\chi^{(1)}(\mathbf{r},\mathbf{r}';\omega_\sigma)$ and the Coulomb potential. In the grid representation, the integral corresponds to a multiplication of matrices of $M\times M$ dimension to an M-dimensional vector. Since the number of grid points M is large, typically 10^4 to 10^5, it is inconvenient to construct the matrix explicitly and to perform the integration

by summing up over the grid points. We instead convert these integrals into equivalent differential equations. The integral involving the Coulomb potential is transformed into the Poisson equation. The integral involving the response function is written as,[26]

$$\int d\mathbf{r}'\chi^{(1)}(\mathbf{r},\mathbf{r}';\omega_\sigma)V(\mathbf{r}') = \sum_i^{occ.} \{\phi_i(\mathbf{r})\psi_i^{(+)}(\mathbf{r}) + \phi_i(\mathbf{r})\psi_i^{(-)}(\mathbf{r})\}, \quad (34)$$

where $\psi_i^{(\pm)}(\mathbf{r})$ are defined by

$$\psi_i^{(\pm)}(\mathbf{r}) \equiv \int d\mathbf{r}' G^{(\pm)}(\mathbf{r},\mathbf{r}';\epsilon_i \pm \hbar\omega_\sigma)V(\mathbf{r}')\phi_i(\mathbf{r}'). \quad (35)$$

The functions $\psi_i^{(\pm)}(\mathbf{r})$ are obtained by solving the following differential equations,

$$(\epsilon_i \pm \hbar\omega_\sigma - h[\rho^{(0)}])\psi_i^{(\pm)}(\mathbf{r}) = V(\mathbf{r})\phi_i(\mathbf{r}). \quad (36)$$

This procedure is known as the modified Sternheimer method.[7,17,26,38] Since we are interested in the responses below the first excited state, the energy $\hbar\omega_\sigma$ is well below the threshold. We therefore take as a boundary condition that the wave function $\psi_i^{(\pm)}(\mathbf{r})$ vanish outside the box. An extension for the response above the threshold is discussed in Ref. 7. In the grid representation, this equation is a linear algebraic equation with sparse, symmetric coefficient matrix. It can be solved efficiently with an iterative method such as the conjugate-gradient (CG) method.[37]

In practical calculations, occupied orbital components in $\psi_i^{(\pm)}(\mathbf{r})$ should be calculated separately in solving Eq. (36) to accelerate the convergence. Namely, we first solve the equation in the space orthogonal to the occupied orbitals,

$$(\epsilon_i \pm \hbar\omega_\sigma - h[\rho^{(0)}])\tilde{\psi}_i^{(\pm)}(\mathbf{r}) = V(\mathbf{r})\phi_i(\mathbf{r}) - \sum_j^{occ.} \phi_j(\mathbf{r})\langle\phi_j|V|\phi_i\rangle. \quad (37)$$

The occupied orbital components are then added,

$$\psi_i^{(\pm)}(\mathbf{r}) = \tilde{\psi}_i^{(\pm)}(\mathbf{r}) + \sum_j^{occ.} \frac{1}{\epsilon_i - \epsilon_j \pm \hbar\omega_\sigma}\phi_j(\mathbf{r})\langle\phi_j|V|\phi_i\rangle. \quad (38)$$

The Sternheimer method is also used to calculate $b^{(n-1)}(\mathbf{r})$ in Eq. (33) which includes integrals involving the higher-order independent particle response functions $\chi^{(2)}$ or $\chi^{(3)}$. To obtain a convergent result (relative residual error of 10^{-10} level), 50 iterations are required for Eq. (37) and 10–20 iterations for Eq. (33). The convergence of iterations are found to become slower and even unstable when the optical frequency comes close to the energy of the first excited state.

Before closing this section, we briefly discuss the computational cost of our method. A detailed consideration of the computational cost of linear response calculations in the real-space method is presented in Ref. 39. We express the number of grid points by M and the number of occupied orbitals by N. For ground-state calculation, the storage requirement scales as $O(MN)$ to store occupied orbitals $\phi_i(\mathbf{r})$. The storage requirement for the response calculation also scales as $O(MN)$ to store $\psi_i^{(\pm)}(\mathbf{r})$. As for the computational time, the orthogonalization procedure has the leading power of $O(MN^2)$ in the ground-state calculation. For small systems, however, the computational time is elapsed mostly in solving the Poisson equation and in the operation of the Hamiltonian. In the response calculation, most time is elapsed in solving the modified Sternheimer equation (37). The leading power is again $O(MN^2)$ coming from the orthogonalization to the occupied orbitals. This number of operations should be multiplied by the number of iterations in solving Eqs. (37) and (33).

TABLE I. Molecular geometries used in the present calculations.

System	Symmetry	
N_2	$D_{\infty h}$	R_{NN}=1.097 68 Å
H_2O	C_{2v}	R_{OH}=0.957 Å, ∠HOH=104.5°
C_2H_4	D_{2h}	R_{CC}=1.34 Å, R_{CH}=1.08 Å, ∠HCH=∠HCC=120°
C_6H_6	D_{6h}	R_{CC}=1.396 Å, R_{CH}=1.083 Å
C_{60}	I_h	R_{C-C}=1.45 Å, $R_{C=C}$=1.39 Å

IV. RESULTS AND DISCUSSION

In this section, we show calculated results of the linear polarizabilities and hyperpolarizabilities with the real-space method. Our purpose here is mainly to confirm reliability of our method to calculate the nonlinear response of molecules and to show the computational feasibility to apply to large molecules. The discussions on the reliability and the limitation of the TD-DFT to describe the nonlinear response are given in detail in Refs. 19, 40, and 41.

All the values shown below are averaged over orientation:

$$\alpha_\parallel = \frac{1}{3}\sum_{i=x,y,z}\alpha_{ii}, \quad (39)$$

$$\beta_\parallel = \frac{1}{5}\sum_{i=x,y,z}(\beta_{zii}+\beta_{izi}+\beta_{iiz}), \quad (40)$$

$$\gamma_\parallel = \frac{1}{15}\sum_{i,j=x,y,z}(\gamma_{iijj}+\gamma_{ijij}+\gamma_{ijji}). \quad (41)$$

The molecular geometries used in our calculations are listed in Table I.

A. Rare-gas atoms (Ne, Ar, Kr)

We show here the calculated hyperpolarizabilities of rare-gas atoms. For a spherically symmetric system, the response equations may be reduced to one-dimensional (1D) equations of radial coordinate. We first performed all-electron calculations in this representation to confirm previous results by Senatore and Subbaswamy,[15] and to set a comparison test for the 3D calculations. For these calculations, we used the simple LDA[31] as was done in Ref. 15, as well as the GGA and LB94 potentials in the radial form. For the 3D calculations, we used the grid representation of wave functions, treating the valence s, p electrons explicitly and core

TABLE II. Polarizabilities $\alpha(-\omega;\omega)$ of rare-gas atoms calculated with several exchange-correlation potentials at $\hbar\omega=1.175$ (eV). See text for the abbreviations of the exchange-correlation potentials. Methods are one-dimensional radial calculation with all electrons (1D-AE), one-dimensional radial calculation with pseudopotential (1D-PP), three-dimensional real-space pseudopotential calculation (3D-RS). Atomic unit is used for the polarizabilities and hyperpolarizabilities in this as well as the following tables.

System	Method	PZ	BLYP	LB94	Expt.[a]
	1D-AE	3.06	3.19	2.60	
Ne	1D-PP	3.18	3.20	3.08	
	3D-RS	3.20	3.23	3.16	2.67
	1D-AE	12.1	12.5	11.5	
Ar	1D-PP	11.9	12.1	12.2	
	3D-RS	12.2	12.3	12.5	11.1
	1D-AE	18.2	18.9	17.1	
Kr	1D-PP	18.4	18.5	19.2	
	3D-RS	18.2	18.4	19.0	16.7

[a]Experimental results from Ref. 42.

electrons by the pseudopotentials. The 3D calculations are achieved with grid points inside a sphere of 8 Å radius and grid spacing of 0.25 Å. With this spatial configuration, the calculated results are found to converge within 1% accuracy. The 1D calculations with the pseudopotentials are shown as well. These results are summarized in Tables II and III. The hyperpolarizabilities of 1D all-electron calculation in the LDA (PZ) coincide precisely with those in Ref. 15.

Comparing measurements and calculations, the linear polarizabilities are described within an accuracy of 10%–15% level. The calculated results do not depend much on the choice of the exchange-correlation potentials. The hyperpolarizabilities, however, depend much on the choice of the exchange-correlation potential. The simple LDA substantially overestimates the THG hyperpolarizability, and the GGA does not improve the discrepancy. The AC potential substantially improves the results, in agreement to the observation in the small molecules.[19]

The calculated results with 1D and 3D methods agree well in general when LDA and GGA potentials are used. This confirms the accuracy of the 3D numerical method, and supports the reliability of the pseudopotentials. The agreement between the 1D and 3D calculations is, however, not very good when the LB94 potential is used. Since the

TABLE III. THG hyperpolarizabilities $\gamma(-3\omega;\omega,\omega,\omega)$ of rare-gas atoms at $\hbar\omega=1.175$ (eV). The abbreviations are the same as for Table II.

System	Method	PZ	BLYP	LB94	Expt.[a]
	1D-AE	232	281	102	
Ne	1D-PP	230	252	129	
	3D-RS	242	270	152	79±8
	1D-AE	2230	2750	1350	
Ar	1D-PP	2260	2690	1610	
	3D-RS	2270	2650	1640	1000±100
	1D-AE	5000	6390	2980	
Kr	1D-PP	5120	6030	3780	
	3D-RS	5100	6020	3890	2790±270

[a]Experimental results by Lehemeier *et al.* (Ref. 43).

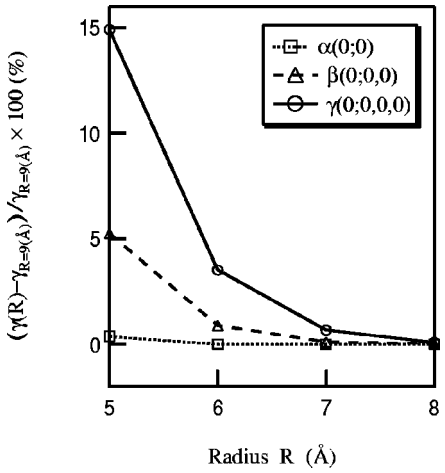

FIG. 1. Convergence of the static linear polarizability and the hyperpolarizabilities of H_2O molecule as to the radius R of the spherical box. Results with $R=9$ Å is regarded as the converged values, and the relative errors are plotted in percent. Spatial mesh size is set to 0.2 Å.

pseudopotential results with 1D and 3D method agree well with each other, this problem does not originate from the computational method but from the inconsistent use of the pseudopotential. The pseudopotential was generated from atomic calculations with LDA exchange-correlation potential. To increase consistency between the construction and the usage of the pseudopotential, the same exchange-correlation potential should be used in the construction and the usage of the pseudopotential. In fact, we found that the hyperpolarizability of Ne atom is 104(a.u.) in the pseudopotential calculation if the pseudopotential is constructed with the LB94 potential, in good agreement with the all-electron calculation. In the following calculations, we show results employing single pseudopotential generated with the LDA potential to simplify the calculations.

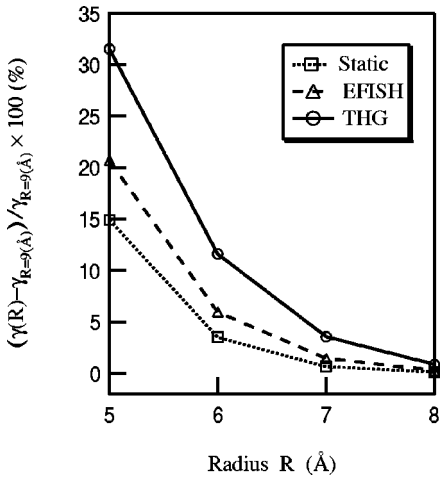

FIG. 2. Convergence of various second hyperpolarizabilities of H_2O molecule as to the radius R of spherical box. Results at $R=9$ Å is regarded as the converged values, and the relative errors are plotted in percent. Spatial mesh size is set to 0.2 Å. The optical frequency is set at $\hbar\omega=1.786$ eV.

TABLE IV. Linear polarizability and hyperpolarizabilities of N_2 molecule. The TD-DFT results for (hyper)polarizabilities calculated with the present real-space method are compared to those with the basis set method. (Refs. 19,12). The real-space calculation is done with a spherical box $R=6$ Å radius and the spatial mesh size $H=0.2$ Å. Coupled cluster calculation [CCSD(T)] and the measurements (Expt.) are also included. The optical frequency is set at $\hbar\omega=1.786$ (eV) for dynamic hyperpolarizabilities.

	Real-Space[a]			Basis[b]				
	VWN	BLYP	LB94	VWN	BLYP	LB94	CCSD(T)[c]	Expt.
$\alpha_\parallel$	12.2	12.3	12.2	12.3		11.5	11.8	11.8[d]
$\gamma_\parallel$	1300	1450	916	1300	1400	769	1010	
EOKE	1370	1540	968	1400	1500	770	1100	
IDRI	1450	1640	1020				1100	
EFISH	1550	1750	1060	1500	1800	840	1100	1057.6 ± 6.4[e]
THG	1880	2150	1250				1300	1295 ± 206[f]

[a]Present method.
[b]Basis set TDDFT calculation by van Gisbergen *et al.* (Refs. 19,12).
[c]Sekino and Bartlett (Ref. 44).
[d]Buckingham *et al.* (Ref. 45).
[e]Mizrahi and Shelton (Ref. 46).
[f]Ward and New (Ref. 47).

B. Small and medium size molecules (N_2, H_2O, C_2H_4, C_6H_6)

We next show results for small molecules. For the dynamic hyperpolarizabilities of small molecules, systematic TD-DFT calculations have been achieved,[19] in which atomic basis functions are employed. By comparing our real-space calculations with them, we can further ascertain the validity of our method and, at the same time, assess the convergence of the previous calculations with respect to the choice of the basis functions.

To illustrate the spatial convergence of our calculation, we show in Fig. 1 the variations of the calculated static (hyper)polarizabilities of water molecule changing the radius of the spherical box. Results employing grid points inside a sphere of 9 Å radius are regarded as converged. The relative differences (in percent) between the results of 9 Å radius and those of smaller radii are plotted. The mesh spacing is fixed at 0.2 Å which is fine enough to get converged results. Comparing the convergence of linear and nonlinear polarizabilities, the larger spatial box is required to obtain a convergent result as the order of nonlinearity increases. This feature corresponds to the usual observation that diffuse basis functions are required for the calculation of hyperpolarizabilities with basis sets.[4] Figure 2 compares convergence of dynamic hyperpolarizabilties for different optical processes. Among them, the larger radius is required for the processes associated with higher optical frequencies. The third harmonic generation, involving the frequency 3ω, shows slowest convergence.

Tables IV, V, VI,and VII summarize results for molecules, N_2, H_2O, C_2H_4, and C_6H_6, respectively. The TD-DFT calculations in the present real-space method are compared with those with basis functions[19] for N_2, H_2O, and C_2H_4 molecules. The same Hamiltonian is used in both cal-

TABLE V. Linear polarizability and hyperpolarizabilities of H_2O molecule. The other features are the same as those of Table IV, except for spatial parameters of real-space calculation. The radius of spherical box is $R=7$ Å and the spatial mesh size is $H=0.2$ Å.

	Real-Space[a]			Basis[b]				
	VWN	BLYP	LB94	VWN	BLYP	LB94	CCSD(T)[c]	Expt.
$\alpha_\parallel$	10.5	10.8	9.64	10.5	10.6	9.20	9.79	9.81[d]
$\beta_\parallel$	−26.1	−27.9	−17.8	−25.7	−27.1	−16.7	−18.0	
OR	−28.6	−30.9	−17.7	−28.1	−29.9	−17.8	−19.0	
SHG	−35.1	−38.8	−20.3	−34.4	−37.3	−20.3	−21.1	-22 ± 0.9[e]
$\gamma_\parallel$	3170	3780	1420	3200	3700	1200	1800	
EOKE	3580	4320	1640	3600	4200	1300	1900	
IDRI	4090	5010	1780				2000	
EFISH	4730	5910	1940	4800	5800	1500	2000	2310 ± 120[e]
THG	8610	12300	2620				2700	

[a]Present method.
[b]Basis set TDDFT calculation by van Gisbergen *et al.* (Refs. 19,12).
[c]Sekino and Bartlett (Ref. 44).
[d]Spackman (Ref. 48).
[e]Ward and Miller (Ref. 49).

TABLE VI. Linear polarizability and hyperpolarizabilities of C_2H_4 molecule. The other features are the same as those of Table IV, except for spatial parameters of real-space calculation. The radius of spherical box is $R=8$ Å and the spatial mesh size is $H=0.25$ Å.

	Real-Space[a]			Basis[b]				
	VWN	BLYP	LB94	VWN	BLYP	LB94	CCSD(T)[c]	Expt.
$\alpha_{\parallel}$	28.3	28.7	28.6	28.7	29.3	27.7	27.1	28.70[d]
$\gamma_{\parallel}$	8850	11 200	5510	8900	11 100	4500	6700	
EOKE	10 200	13 100	6090	10 500	13 000	5000	7700	
IDRI	11 800	15 800	6770				8800	
EFISH	14 000	19 200	7580	14 000	19 400	6100	10 200	9030 ± 200[e]
THG	26 800	46 100	11 300				18 200	

[a]Present method.
[b]Basis set TDDFT calculation by van Gisbergen *et al.* (Refs. 19,12).
[c]Sekino and Bartlett (Ref. 44).
[d]Bose and Cole (Ref. 50).
[e]Ward and Elliott (Ref. 51).

culations except for the use of the pseudopotential in the present calculation. The coupled cluster calculations by Sekino and Bartlett,[44] as well as the experimental values are also included.

The agreement between two TD-DFT calculations is generally good, within a few percent for VWN and BLYP potentials. This confirms again the usefulness of our method to calculate hyperpolarizabilities. The results with LB94 disagrees as large as 20%. This originates from the inconsistent use of the pseudopotential in the present calculation as we mentioned before in the rare-gas calculation. In the all-electron calculation of Ref. 19, the gradient correction in the LB94 utilizes electron density, which includes the core electron density. In the present pseudopotential calculation, however, the core electron density is not included.

In Table VII we show results of benzene molecule as an example of a medium size molecule. We made calculations in a spherical box with 8 Å radius and 0.25 Å grid-spacing, which are enough to get converged results within a few percent accuracy. For molecules of this size, the difference of the second hyperpolarizability among the different exchange-correlation potentials becomes gradually less significant.

Although linear polarizability does not depend much on the choice of the exchange-correlation potential, hyperpolarizabilities are rather sensitive. Since the different exchange-correlation potentials are employed only in the ground-state calculations and the same ALDA kernel is used in the response equations, this strong dependence on the exchange-correlation potential originates from the quality of the ground states description. As was noticed by Ref. 19, the AC potential such as LB94 improves the results considerably. Since the TD-DFT is a convenient scheme to calculate nonlinear optical responses of large systems, further improvements of the exchange-correlation potential are very much needed.[40,41]

C. C_{60}

Finally we present real-space calculation of C_{60} molecule as an example of a large system. In Fig. 3, second hyperpolarizabilities of C_{60} molecules calculated with different spatial parameters are plotted. The converged result is obtained with a spherical box size of 10 Å radius and a grid spacing of 0.3 Å.

TABLE VII. Linear polarizability and hyperpolarizabilities of benzene molecule. The real-space TD-DFT calculation is done with a spherical box $R=8$ Å radius and the spatial mesh size $H=0.25$ Å. Other static LDA result, TDHF result and experimental results are also shown.

		Real-Space[a]			Basis[b]		
	$\hbar\omega$ (eV)	VWN	BLYP	LB94	LDA	TDHF[c]	Expt.
$\alpha_{\parallel}$	static	70.2	70.8	71.5	72.2	62.6	67.5[d]
$\gamma_{\parallel}$	static	19 000	23 800	12 900	22 000	15 200	
EOKE	1.786	21 800	28 000	14 400		17000	
IDRI	2.06	28 800	39 000	17 500		21 300	
EFISH	1.786	30 400	41 400	18 200		21 800	$24\,500\pm600$ (gas)[f]
EFISH	1.165	22 800	29 400	14 800		17 600	$17\,750\pm190$ (gas)[g], $27\,900\pm4200$ (liq.)[h]
THG	0.656	21 200	27 100	14 100		16 700	$29\,000\pm8600$ (liq.)[i]

[a]Present method.
[b]Quong and Pederson (Ref. 52).
[c]Karna *et al.* (Ref. 53).
[d]Boggard *et al.* (Ref. 54).
[e]Ward and Elliott (Ref. 51).
[f]Kaatz *et al.* (Ref. 55).
[g]Levine and Bethea (Ref. 56).
[h]Hermann (Ref. 57).

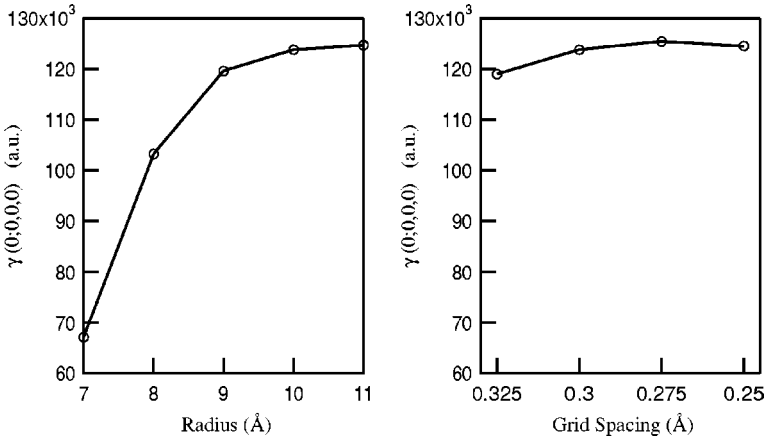

FIG. 3. Convergence of the static second hyperpolarizability of C_{60} molecule with respect to the radius R of spherical box and the grid-spacing H. $H=0.3$ Å is used in the left panel and $R=10$ Å in the right panel.

In Table VIII, real-space TD-DFT results are compared with results of basis set TD-DFT calculation, other *ab initio* calculations, and experimental results. Our result for the static second hyperpolarizability in the LDA is about 35% larger than that in the basis set calculation reported in Ref. 18. In view of a good agreement between our real-space and basis function calculations for other molecules, we believe that the difference may be due to an insufficient basis set in the calculation using an atomic basis set.

As was discussed in Ref. 18, experimental results are more than one order of magnitude larger than the theoretical value. The experimental difficulty in determining the hyperpolarizability of C_{60} was discussed in Ref. 62. An upper limit for the hyperpolarizability of C_{60} has been reported in Ref. 62. The result, $\gamma<437\,000$ (a.u.), is consistent with the TD-DFT and the other *ab initio* results.

V. SUMMARY

We have developed a real-space computational method for dynamic hyperpolarizabilities in the time-dependent density functional theory. The method is based on the response function formalism developed by Senatore and Subbaswamy.[15] The modified Sternheimer method[26] is used to convert the integral equations into the equivalent differential equations. These equations are discretized employing a uniform grid representation in a three-dimensional Cartesian coordinate, and are solved with efficient iterative methods such as the conjugate-gradient and conjugate-residual methods.

The present method can be applied to any kind of nonlinear optical processes of molecules up to third order. One of the preferable features of the present method, in comparison with the standard methods employing basis functions, is a convenience to confirm the convergence of the calculation as to the spatial configurations which are specified by two intuitive parameters, the grid spacing and the spatial extension of grid points. In the present method, we can obtain converged results for the hyperpolarizabilities of molecules as large as C_{60}.

We made calculations of hyperpolarizabilities of rare-gas atoms, small and medium size molecules, and C_{60} as an example of large molecules. Several exchange-correlation potentials are used including conventional LDA, gradient correction, and asymptotically corrected one (LB94). The calculated hyperpolarizabilities agree accurately with those calculated with other methods for small and medium size molecules. Slight differences are observed, however, when one uses the LB94 potential. This originate from the difference of the gradient of the density in the core region between the all-electron and the present pseudopotential calculations. For C_{60}, our converged value of the hyperpolarizability is somewhat larger than that calculated with the basis function

TABLE VIII. Linear polarizability and hyperpolarizabilities of C_{60} molecule. The TD-DFT results for hyperpolarizabilities calculated with the present real-space method are compared to those with the basis set method Ref. 19 and other *ab initio* method Ref. 58. The real-space calculation is done with a spherical box $R=10$ Å radius and the spatial mesh size $H=0.3$ Å.

		Real-Space[a]			Basis[b]			
	$\hbar\omega$ (eV)	VWN	BLYP	LB94	LDA	LB94	DD-CRPA[c]	Expt.
$\alpha_{\parallel}$	static	541	545	544	557	544	508	596[d]
$\gamma_{\parallel}$	static	124 000	152 000	94 300	87 400	65500	114000	
EOKE	1.5	145 000	181 000	110 000		79700		
IDRI	1.165	159 000	197 000	119 000				$<60\times\gamma_{\text{benzene}}$[e]
EFISH	0.65	134 000	166 000	102 000		72000		8 930 000[f]
THG	0.52	138 000	170 000	105 000				340 000±50 000[d]

[a]Present method.
[b]van Gisbergen *et al.* (Ref. 18).
[c]Norman *et al.* (Ref. 58).
[d]Meth *et al.* (Ref. 59).
[e]Tang *et al.* Ref. 60).
[f]Wang and Cheng (Ref. 61).

method, likely because of the insufficiency of the basis functions employed.

The real-space method presented in this paper thus offers a new computational approach for the nonlinear optical response of molecules. Although the applicability is limited to the TD-DFT in which the correlation effects are included through local exchange-correlation potential, the method works efficiently both for small and large molecules and allows us to obtain results convergent with respect to spatial configurations.

As pointed out previously, the hyperpolarizabilities in the TD-DFT calculation depends much on the choice of the exchange-correlation potential in the ground-state calculation. The asymptotically corrected potential, which is known to describe rather accurately the excited-state properties of molecules, gives results closest to the measurements among the potentials. Since the present method is an efficient new method to calculate molecular hyperpolarizabilities, we hope to apply it in exploring molecules of practical interest with large nonlinearity. For that purpose, it is also necessary to pay further efforts to improve the exchange-correlation potential.[41]

ACKNOWLEDGMENTS

This work was supported by the Ministry of Education, Culture, Sports, Science and Technology of Japan, Contract No. 11640372. The authors acknowledge the Institute of Solid State Physics, University of Tokyo, and the Institute of Physical and Chemical Research, for the use of supercomputers.

[1] J. L. Brédas, C. Adant, P. Tackx, and A. Persoons, Chem. Rev. **94**, 243 (1994).
[2] D. P. Shelton and J. E. Rice, Chem. Rev. **94**, 3 (1994).
[3] K. Ohta, T. Sakaguchi, K. Kamada, and T. Fukumi, Chem. Phys. Lett. **274**, 306 (1997).
[4] T. Pluta and A. J. Sadlej, Chem. Phys. Lett. **297**, 391 (1998).
[5] E. K. U. Gross, J. F. Dobson and M. Petersilka, in *Density Functional Theory*, Springer Series Topics in Current Chemistry, edited by R. F. Nalewajski (Springer, Heidelberg, 1996), p. 81.
[6] M. E. Casida, C. Jamorski, K. C. Casida, and D. R. Salahub, J. Chem. Phys. **108**, 4439 (1998).
[7] T. Nakatsukasa and K. Yabana, J. Chem. Phys. **114**, 2550 (2001).
[8] A. Zangwill and P. Soven, Phys. Rev. A **21**, 1561 (1980).
[9] K. Yabana and G. F. Bertsch, Phys. Rev. B **54**, 4484 (1996).
[10] K. Yabana and G. F. Bertsch, Int. J. Quantum Chem. **75**, 55 (1999).
[11] G. F. Bertsch, J.-I. Iwata, A. Rubio, and K. Yabana, Phys. Rev. B **62**, 7998 (2000).
[12] S. J. A. van Gisbergen, V. P. Osinga, O. V. Gritsenko, R. van Leeuwen, J. G. Snijders, and E. J. Baerends, J. Chem. Phys. **105**, 3142 (1996).
[13] T. Kirchner, L. Gulyas, H. J. Lüdde, E. Engel, and R. M. Dreizler, Phys. Rev. A **58**, 2063 (1998).
[14] R. Nagano, K. Yabana, T. Tazawa, and Y. Abe, Phys. Rev. A **62**, 062721 (2000).
[15] G. Senatore and K. R. Subbaswamy, Phys. Rev. A **35**, 2440 (1987).
[16] Z. H. Levine, Phys. Rev. B **49**, 4532 (1994).
[17] A. D. Corso, F. Mauri, and A. Rubio, Phys. Rev. B **53**, 15638 (1996).
[18] S. J. A. van Gisbergen, J. G. Snijders, and E. J. Baerends, Phys. Rev. Lett. **78**, 3097 (1997).
[19] S. J. A. van Gisbergen, J. G. Snijders, E. J. Baerends, J. Chem. Phys. **109**, 10644 (1998); , **109**, 10657 (1998); (erratum) **111**, 6652 (1999).
[20] J. R. Chelikowsky, N. Troullier, K. Wu, and Y. Saad, Phys. Rev. B **50**, 11355 (1994).
[21] T. L. Beck, Rev. Mod. Phys. **72**, 1041 (2000).
[22] E. L. Briggs, D. J. Sullivan, and J. Bernholc, Phys. Rev. B **54**, 14362 (1996).
[23] A. D. Becke, Int. J. Quantum Chem., Quantum Chem. Symp. **23**, 599 (1989).
[24] R. M. Dickson and A. D. Becke, J. Phys. Chem. **100**, 16105 (1996).
[25] I. Vasiliev, S. Ögüt, and J. R. Chelikowsky, Phys. Rev. Lett. **82**, 1919 (1999).
[26] G. D. Mahan, Phys. Rev. A **22**, 1780 (1980).
[27] J.-I. Iwata, K. Yabana, and G. F. Bertsch, Nonlinear Optics **26**, 9 (2000).
[28] P. N. Butcher and D. Cotter, *The Elements of Nonlinear Optics* (Cambridge University Press, Cambridge, 1990).
[29] N. Troullier and J. Martins, Phys. Rev. B **43**, 1993 (1991).
[30] L. Kleinman and D. Bylander, Phys. Rev. Lett. **48**, 1425 (1982).
[31] J. P. Perdew and A. Zunger, Phys. Rev. B **23**, 5048 (1981).
[32] S. H. Vosko, L. Wilk, and M. Nusair, Can. J. Phys. **58**, 1200 (1980).
[33] A. D. Becke, Phys. Rev. A **38**, 3098 (1988).
[34] C. L. Lee, W. Yang, and R. G. Parr, Phys. Rev. B **37**, 785 (1988).
[35] R. van Leeuwen and E. J. Baerends, Phys. Rev. A **49**, 2421 (1994).
[36] M. E. Casida, K. C. Casida, and D. R. Salahub, Int. J. Quantum Chem. **70**, 933 (1998).
[37] R. Barrett *et al.*, *Templates for the Solution of Linear Systems: Building Blocks for Iterative Methods* (Society for Industrial and Applied Mathematics, Philadelphia, 1994).
[38] X. Gonze, Phys. Rev. A **52**, 1096 (1995).
[39] G. F. Bertsch, A. Rubio, and K. Yabana (unpublished).
[40] S. J. A. van Gisbergen, F. Kootstra, P. R. T. Schipper, O. V. Gritsenko, J. G. Snijders, and E. J. Baerends, Phys. Rev. A **57**, 2556 (1998).
[41] P. R. T. Schipper, O. V. Gritsenko, S. J. A. van Gisbergen, and E. J. Baerends, J. Chem. Phys. **112**, 1344 (2000).
[42] P. J. Leonard, At. Data Nucl. Data Tables **14**, 21 (1974).
[43] H. T. Lehemeier, W. Leupacher, and A. Penzkofer, Opt. Commun. **56**, 67 (1985).
[44] H. Sekino and R. Bartlett, J. Chem. Phys. **98**, 3022 (1993).
[45] A. D. Buckingham, M. P. Bogaard, D. A. Dunmur, C. Hobbs, and B. J. Orr, Trans. Faraday Soc. **66**, 1548 (1970).
[46] Y. Mizrahi and D. P. Shelton, Phys. Rev. Lett. **55**, 696 (1985).
[47] J. F. Ward and G. H. C. New, Phys. Rev. **185**, 57 (1969).
[48] M. A. Spackman, J. Phys. Chem. **93**, 7594 (1989).
[49] J. F. Ward and C. K. Miller, Phys. Rev. A **19**, 826 (1979).
[50] T. K. Bose and R. H. Cole, J. Chem. Phys. **54**, 3829 (1971).
[51] J. F. Ward and D. S. Elliott, J. Chem. Phys. **69**, 5438 (1978).
[52] A. A. Quong and M. R. Pederson, Phys. Rev. B **46**, 12906 (1992).
[53] S. P. Karna, G. B. Talapatra, and P. N. Prasad, J. Chem. Phys. **95**, 5873 (1991).
[54] M. P. Boggard, A. D. Bucknghan, M. G. Corfield, D. A. Dunmur, and A. H. White, Chem. Phys. Lett. **12**, 558 (1972).
[55] P. Kaatz, E. A. Donley, and D. P. Shelton, J. Chem. Phys. **108**, 849 (1998).
[56] B. F. Levine and C. G. Bethea, J. Chem. Phys. **63**, 2666 (1975).
[57] J. P. Harmann, Opt. Commun. **9**, 74 (1973).
[58] P. Norman, Y. Luo, D. Jonsson, and H. Ågren, J. Chem. Phys. **106**, 8788 (1997).
[59] J. S. Meth, H. Vanherzeele, and Y. Wang, Chem. Phys. Lett. **197**, 26 (1992).
[60] N. Tang, J. P. Partanen, R. W. Hellwarth, and R. J. Knize, Phys. Rev. B **48**, 8404 (1993).
[61] Y. Wang and L.-T. Cheng, J. Phys. Chem. **96**, 1530 (1992).
[62] L. Geng, and J. C. Wright, Chem. Phys. Lett. **249**, 105 (1996).